Observations of Near-Surface Current Shear Help Describe Oceanic Oil and Plastic Transport

Nathan J. M. Laxague, Tamay M. Ö-Zgökmen, Brian K. Haus, Guillaume Novelli, Andrey Shcherbina, Peter Sutherland, Cédric M. Guigand, Björn Lund, Sanchit Mehta, Matias Alday, et al.

AGU PUBLICATIONS

Geophysical Research Letters

RESEARCH LETTER
10.1002/2017GL075891

Key Points:
- The current profile is measured over the upper few centimeters of the ocean
- Profound shear is observed over the upper decimeter
- This results in differential transport of debris by size and buoyancy

Supporting Information:
- Supporting Information S1

Correspondence to:
N. J. M. Laxague,
nl2623@columbia.edu

Citation:
Laxague, N. J. M., Özgökmen, T. M., Haus, B. K., Novelli, G., Shcherbina, A., Sutherland, P., … Molemaker, J. (2018). Observations of near-surface current shear help describe oceanic oil and plastic transport. *Geophysical Research Letters*, *45*, 245–249. https://doi.org/10.1002/2017GL075891

Received 30 SEP 2017
Accepted 26 NOV 2017
Accepted article online 4 DEC 2017
Published online 8 JAN 2018

Observations of Near-Surface Current Shear Help Describe Oceanic Oil and Plastic Transport

Nathan J. M. Laxague[1], Tamay M. Özgökmen[1], Brian K. Haus[1], Guillaume Novelli[1], Andrey Shcherbina[2], Peter Sutherland[3], Cédric M. Guigand[1], Björn Lund[1], Sanchit Mehta[1], Matias Alday[3], and Jeroen Molemaker[4]

[1]Department of Ocean Sciences, Rosenstiel School of Marine and Atmospheric Science, University of Miami, Miami, FL, USA, [2]Applied Physics Laboratory, University of Washington, Seattle, WA, USA, [3]Laboratoire d'Oceanographie Physique et Spatiale, L'Institut Francais de Recherche pour l'Exploitation de la Mer, Centre Bretagne, Plouzané, France, [4]Atmospheric and Oceanic Sciences, University of California Los Angeles, Los Angeles, CA, USA

Abstract Plastics and spilled oil pose a critical threat to marine life and human health. As a result of wind forcing and wave motions, theoretical and laboratory studies predict very strong velocity variation with depth over the upper few centimeters of the water column, an observational blind spot in the real ocean. Here we present the first-ever ocean measurements of the current vector profile defined to within 1 cm of the free surface. In our illustrative example, the current magnitude averaged over the upper 1 cm of the ocean is shown to be nearly four times the average over the upper 10 m, even for mild forcing. Our findings indicate that this shear will rapidly separate pieces of marine debris which vary in size or buoyancy, making consideration of these dynamics essential to an improved understanding of the pathways along which marine plastics and oil are transported.

1. Introduction

Two of the Earth's great fluid reservoirs, the oceans and the atmosphere, meet at the sharp discontinuity of the air-sea interface. Pieces of buoyant marine debris tend to accumulate at this boundary (Matthews et al., 2017); this is especially true for the most massive among them (Reisser et al., 2015). However, neither observations nor operational ocean models resolve the ocean current profile in the upper few centimeters of the sea, where motion is primarily determined by wind forcing and wave dynamics (Wu, 1983). Most prominent among these effects is Stokes drift (Stokes, 1847), the depth-decaying net forward motion that results from wave orbital velocities. Difficulty in observing this current shear arises from disturbance of the flow by measurement systems and the challenge of extracting physical information near to an undulating boundary, resulting in an observational gap. This blind spot is not trivial—although motion in this layer occupies a miniscule share of overall volumetric flow—it has a dominant impact on buoyant material transport. As an example, microplastics (characteristic size $d < 5$ mm), the most ecologically damaging of buoyant marine debris (Wright et al., 2013), generally have low rise velocities and are found throughout the water column (Kukulka et al., 2012). Concentrations of mesoplastic (5 mm $< d <$ 25 mm) and macroplastic ($d >$ 25 mm), however, sharply decay with depth (Reisser et al., 2015). Based on comprehensive plastic sampling of open ocean and coastal waters (Cooper & Corcoran, 2010; Isobe et al., 2014), it is understood that one important pathway involves the transport of macroplastic and mesoplastic to coastal margins by wind/wave-induced near-surface currents and subsequent fragmentation in the surfzone. The resulting microplastics have small rise velocities and therefore distribute themselves deeper in the water column; at greater depths, these fragments will not be preferentially transported to the shore by rapid, near-surface currents. Surface-dwelling spilled oil presents an additional concern to ecosystem and human health. The density of crude oil compounds may vary substantially within a given volume; however, the portions floating nearest to the surface have the greatest chance of interacting with marine wildlife and the strongest likelihood of reaching shorelines, at which point their potential to harm humans and wildlife is greatest (Wolfe et al., 1994). Predictive models that directly couple the ocean and atmosphere (Curcic et al., 2016) or impose wind and wave-resulting drift on top of Eulerian flow (Le Hénaff et al., 2012) are an important intermediate step in the efforts to describe this material transport despite their inability to resolve centimeter-depth dynamics. Recent findings (Iwasaki et al., 2017) indicate

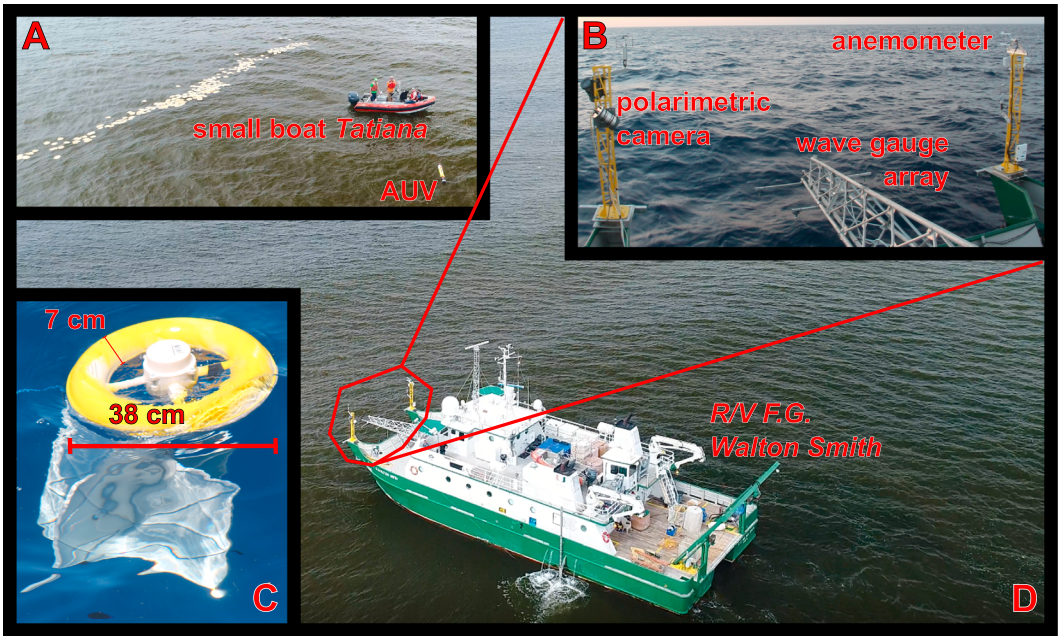

Figure 1. Images of *R/V F.G. Walton Smith* and observational tools: (a) Close-up of bamboo plates in wind row adjacent to the small boat Tatiana. (b) View of bow-mounted instruments. (c) Close-up of GPS-tracked drifter, with white drogue visible below surface. (d) Drone shot of *R/V F.G. Walton Smith*.

that incorporating Stokes drift into ocean circulation models (even at 1 m vertical resolution) fundamentally changes transport patterns near coastal margins. Another modeling study (Le Hénaff et al., 2012) performed in the wake of the Deepwater Horizon disaster suggested that near-surface wind and wave-induced currents were one of the principal reasons that surface oil was kept in the northern Gulf of Mexico (and away from the Loop Current, which would have connected it to the Florida Current and on to the Gulf Stream).

2. Materials and Methods

In order to shed light on the hydrodynamics of the near-surface layer of the ocean, a dedicated observational experiment (explained in greater detail within the supporting information) was conducted in the northern Gulf of Mexico aboard the Research Vessel *F.G. Walton Smith* for over three and a half hours on 27 April 2017 as part of the 2 week long SPLASH (Submesocale Processes and Lagrangian Analysis on the SHelf) research campaign. The experiment was designed with the intent of combining the complementary strengths of disparate platforms and techniques. Specifically, acoustic Doppler current profilers (ADCPs) are unable to reliably recover the current vector profile near to an undulating boundary, a result of side-lobe contamination (Cole & Symonds, 2015). This blind spot is filled in here through a combination of drifting instruments and near-field remote sensing that target near-surface flows while missing the deeper currents described by the ADCP. These devices and techniques were used in parallel in order to recover the high-resolution current velocity profile between 1 cm and the seabed at 13.5 m below the surface, ultimately allowing for isolation of the forcing mechanisms over the full depth range. The sensors and instruments used included drone-tracked bamboo plates, GPS-tracked drogued and undrogued drifters (Novelli et al., 2017), a polarimetric camera (Zappa et al., 2008; Laxague et al., 2017), an autonomous vehicle-mounted acoustic Doppler current profiler (ADCP), a shipboard ADCP, a bow-mounted array of sonic wave gauges (Donelan et al., 1996), and a mast-mounted sonic anemometer. The wave number spectra produced from the sonic wave gauge array and polarimeteric camera data were combined in order to produce a single directional spectrum, which described waves from gravity to pure capillary scales ($0.1<k<10,00$ rad/m, wavelength ranging from 6.28 mm to 62.8 m); the Stokes drift vector profile was computed from this composite spectrum (Webb & Fox-Kemper, 2015). Local homogeneity in the wave field was assumed at least within the wave gauge footprint of ≈ 4 m^2; at larger scales, wave conditions did not vary greatly across the spatiotemporal extent of the observations. The bamboo plates had drafts of 1.75 cm, while the undrogued and drogued drifters had drafts of 3.5 cm and 70 cm (the latter having a center of drag at 30 cm depth), respectively. These devices are shown in Figure 1; their drift speeds are

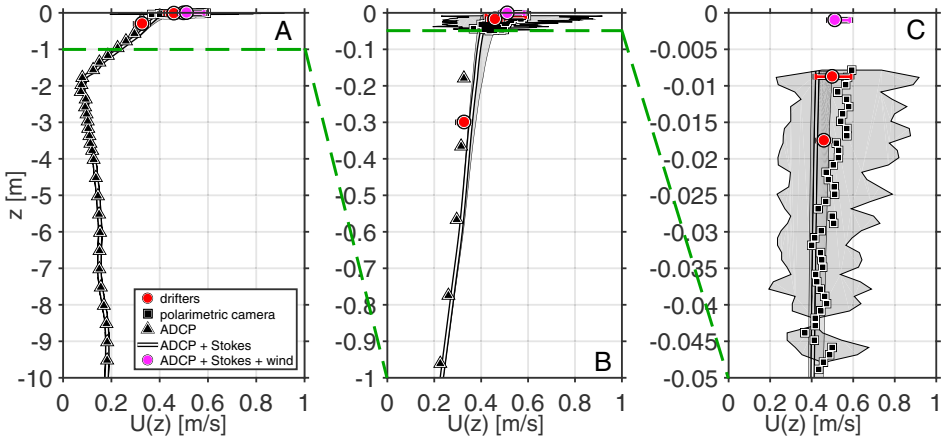

Figure 2. Full observed current profile: Current magnitudes are shown at depths of (a) 10 m, (b) 1 m, and (c) 0.05 m. Green dashed lines indicate the "zooming in" progression from Figures 2a–2c. Symbols: triangles, ADCP; squares, polarimetric camera (Laxague et al. (2017), with depth assigned following Plant and Wright (1980)); line, Stokes drift (Webb & Fox-Kemper, 2015) plus ADCP current; magenta circle, Stokes drift plus ADCP current plus empirical 8.5 cm/s "interface forcing" drift (Wu, 1983); and red circles, centroid speeds of bamboo plates and drifters. Shaded regions (polarimetric current, Stokes drift plus ADCP) and horizontal bars (drifting instruments) define the 5th–95th percentile range. The darker shaded region in Figure 2c represents the 5th–95th percentile range of the Stokes drift and corresponds to the shaded region around the wave spectrum shown in Figure S3 of the supporting information. Note that the drifter centroid depths Z indicate the center of an average over $-2Z < z < 0$ and not a true point measurement.

given in Figure 2 (with the direction of the drift given in supporting information Figure S1b). The sum of the ADCP and Stokes drift profiles is a surface-extrapolated Lagrangian current profile; the drifting objects provide observational points of comparison within the ocean's upper decimeters. The plates, which were initially randomly and uniformly distributed over a 100 m diameter patch of the ocean, formed into a linear feature consistent with a windrow (Figure 1), a phenomenon seen in nearly all surface-following material under the influence of wind and waves (Jones et al., 2016). Drifters were deployed in a ring around this patch. Given the arrangement of the plates and undrogued drifters along windrows, it is expected that they moved quicker than they would outside of those local convergence zones. Despite this apparent bias in the measurement, such an observation is quite relevant to the study of material transport in the upper centimeters of the ocean. For the purposes of this study, all profiles shown are representative of the mean over the three and a half-hour observation period. The time-varying drifter speeds and polarimetric current magnitudes are shown in Figure S2 of the supporting information.

3. Results

Environmental conditions at the time and place of measurement were well suited for the delineation of wind-induced, wave-induced, and pressure gradient-induced flows at different levels of the water column, making it an ideal case for study. Subsurface southeastward flow (≈20 cm/s magnitude) was oriented nearly orthogonally to the southwestward wind velocity and wave direction. The observed wind speed—corrected to a 10 m reference level and neutral stratification—was 4.3 m/s, the dominant wave period was 1.9 s, and the significant wave height was 0.86 m. Upper ocean density stratification was found to be negligible to an ≈8 m mixed layer depth (supporting information Figure S1c).

The drifting instruments and polarimetric camera observed the full Lagrangian near-surface current, a combination of background Eulerian flow, Stokes drift, and the sum of microscale wave breaking and skin friction. The latter will hereafter be referred to as "interface forcing"; it is a significant mediator of momentum transfer between the atmosphere and the ocean (Sutherland & Melville, 2013). Its relevance to the present topic is central, as it results in a layer of strong turbulence and high shear in the top few centimeters of the water column (Sutherland & Melville, 2015). By separately evaluating the Stokes drift and comparing the interface forcing with classic parameterization, we delineate the flow into its constituent elements. The sum of the empirical Stokes drift profile (Webb & Fox-Kemper, 2015) and the ADCP-sensed background Eulerian current profile yields near-surface currents that are of smaller magnitude than those measured by the drifting

Table 1
Comparison of Drift Speeds by Depth Range Averaged by Each Instrument: Drift Speed, Direction, and Distance for Averages Over Layers of Six Different Thicknesses of the Observed Current Velocity Profile

Segment	Thickness of layer (m)	Measured by	Speed (m/s)	Direction (deg)	Drift distance after 1 day (km)
A	0.01	Surface tracers	0.57 ± 0.01	242 ± 2	49 ± 1
B	0.10	Polarimetric camera, drifters	0.43 ± 0.07	250 ± 14	37±6
C	0.50	Drifters, ADCP	0.35 ± 0.05	245 ± 13	30 ± 4
D	1.00	ADCP	0.30 ± 0.06	231 ± 11	26 ± 5
E	2.00	ADCP	0.22 ± 0.10	219 ± 14	19 ± 9
F	10.00	ADCP	0.16 ± 0.05	162 ± 40	14 ± 4

Note. The error margins given (e.g., 0.57 ± 0.01) represent 1 standard deviation from the mean. Also, included are the segment labels (A–F) corresponding to Figure 3 and the observational and modeling tools which are able to resolve each layer. The mean wind velocity direction was 242°.

instruments and polarimetric camera. A series of classic laboratory studies of surface drift (Wu, 1983) found that interface forcing should scale like $0.53u_*$, where u_* is the air-side friction velocity. For this case, the u_* computed from the observed wind stress was 16.0 cm/s, corresponding to an estimated wind drift of ≈8.5 cm/s. Adding this quantity to the nearest-surface element of the Stokes drift estimate (Webb & Fox-Kemper, 2015) and the background Eulerian flow, we obtain a drift speed within 2.5% of the mean plate drift speed and 5% of the mean nearest-surface polarimetric current (Figure 2). This suggests that the nearest-surface difference between the camera-determined current profile and the extrapolated ADCP + Stokes profile is accounted for by interface forcing.

Considerable ambiguity exists regarding the definition of the depth at which ocean "surface" currents are found—each of the vertical layers listed in Table 1 has been taken as such in observational or modeling literature in recent years. The mean value of our computed Stokes drift profile over the upper 1 m is 4.9 cm/s or 31% of u_*. This is consistent with the literature range (Ardhuin et al., 2009) of 16–35% of u_*. However, the velocity profile is strongly sheared with depth—each "zooming in" step from Figures 2a–2c shows increasingly strong shear as one gets nearer to the air-sea interface. This results in a quantifiably profound impact upon the direction and distance of centimeter-scale buoyant material transport: the current speed at 1 cm is twice that of the average speed over the upper 1 m and nearly four times that of the average speed over the upper 10 m (Figures 2 and 3). In comparing the plastic distribution shown on the margin of Figure 3 with transport estimates given in Table 1, it is evident that capturing the dynamics of the upper decimeter of the ocean is essential to describing the movement of marine plastics.

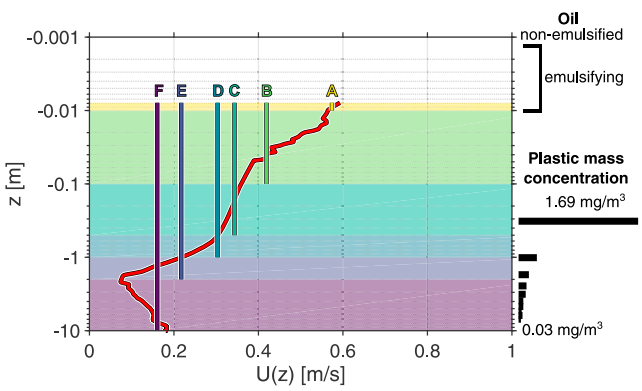

Figure 3. Current magnitude and material distribution: Red line indicates composite profile generated using all observational data. Labels A–F marking colored layers and vertical lines correspond to ranges given in Table 1. Representation of material distribution is given on right margin. The uppermost layers hold nonemulsified (≈1 mm) and emulsifying/emulsified (≈1 cm) oil (Daling et al., 2003). Plastic concentration (Reisser et al., 2015) is represented by the black bars, with length proportional to concentration as indicated above and below them.

4. Discussion

Although it is understood that marine debris tends to collect inside the large ocean subtropical (anticyclonic) gyres (Cózar et al., 2014; Law et al., 2010; Maximenko et al., 2012), many of the specific mechanisms responsible for the degradation of macromesoplastic and mesoplastic occur away from these areas of convergence (Iwasaki et al., 2017). The present work offers compelling observations of strong near-surface current shear, implying that macromesoplastic and mesoplastic are predominantly transported by wind and wave-induced motions which strongly diverge from currents at greater depths. This results in size-dependent differential transport, which is an essential segment in the time line of a piece of oceanic plastic. Additionally, spilled oil often emulsifies and distributes itself throughout the water column (Jones et al., 2016), though it is generally surface-residing oil slicks which most severely harm marine wildlife in the open ocean and carry the greatest likelihood of reaching coastal margins (Wolfe et al., 1994). Given the observations presented here, material transport is likely to be poorly estimated by models that neglect or cannot sufficiently parameterize wind or wave-related motions and do not

have sufficient resolution to describe this thin near-surface layer. We show that currents in the upper few centimeters of the ocean may have drastically different magnitudes and directions than the average over the upper meter, a vertical extent commonly taken as the thickness of the ocean's surface layer. As a result, incorporation of these dynamics into forecasting efforts will be an essential component of the community's mission to better understand the movement of ocean plastics and the fate of spilled oil.

Acknowledgments
The authors declare no competing financial interests. N. J. M. L. serves without monetary compensation as board member and Director of Science for the nonprofit organization Debris Free Oceans (http://debrisfreeoceans.org). This research was made possible by grant SA1207-GOMRI005 from the Gulf of Mexico Research Initiative. Data are publicly available through the Gulf of Mexico Research Initiative Information and Data Cooperative (GRIIDC) at https://data.gulfresearchinitiative.org/data/R4.x265.000:0038 (DOI: 10.7266/N7ZW1JC0). Thanks are given to all those who aided in data collection, particularly Neil Williams and Trina Litchendorf. The authors thank the captain and crew of the *R/V F.G. Walton Smith* for their hard work and careful execution. Finally, N. J. M. L. thanks Bill Plant for his role in shaping the method by which currents were inferred from the characteristics of gravity-capillary waves.

References

Ardhuin, F., Mari, L., Rascle, N., Forget, P., Roland, A., Ardhuin, F., … Roland, A. (2009). Observation and estimation of Lagrangian, Stokes, and Eulerian currents induced by wind and waves at the sea surface. *Journal of Physical Oceanography*, *39*(11), 2820–2838. https://doi.org/10.1175/2009JPO4169.1

Cole, R., & Symonds, D. (2015). A 25 year collaboration using ADCPs. In *2015 IEEE/OES 11th Current, Waves and Turbulence Measurement (CWTM)* (pp. 1–10). St. Petersburg, FL, USA: IEEE - Institute of Electrical and Electronics Engineers, Inc. https://doi.org/10.1109/CWTM.2015.7098110

Cooper, D. A., & Corcoran, P. L. (2010). Effects of mechanical and chemical processes on the degradation of plastic beach debris on the island of Kauai, Hawaii. *Marine Pollution Bulletin*, *60*(5), 650–654. https://doi.org/10.1016/j.marpolbul.2009.12.026

Cózar, A., Echevarría, F., González-Gordillo, J. I., Irigoien, X., Úbeda, B., Hernández-León, S., … Karl, D. M. (2014). Plastic debris in the open ocean. *Proceedings of the National Academy of Sciences*, *111*(28), 10,239–10,244. https://doi.org/10.1073/pnas.1314705111

Curcic, M., Chen, S. S., & Özgökmen, T. M. (2016). Hurricane-induced ocean waves and stokes drift and their impacts on surface transport and dispersion in the Gulf of Mexico. *Geophysical Research Letters*, *43*, 2773–2781. https://doi.org/10.1002/2015GL067619

Daling, P. S., Moldestad, M. Ø., & Johansen, Ø. (2003). Norwegian testing of emulsion properties at sea: The importance of oil type and release conditions. *Spill Science and Technology Bulletin*, *8*(1), 123–136. https://doi.org/10.1016/S1353-2561(03)00016-1

Donelan, M. A., Drennan, W. M., & Magnusson, A. K. (1996). Nonstationary analysis of the directional properties of propagating waves. *Journal of Physical Oceanography*, *26*(9), 1901–1914. https://doi.org/10.1175/1520-0485(1996)026<1901:NAOTDP>2.0.CO;2

Isobe, A., Kubo, K., Tamura, Y., Kako, ichio, Nakashima, E., & Fujii, N. (2014). Selective transport of microplastics and mesoplastics by drifting in coastal waters. *Marine Pollution Bulletin*, *89*, 324–330. https://doi.org/10.1016/j.marpolbul.2014.09.041

Iwasaki, S., Isobe, A., Kako, S., Uchida, K., & Tokai, T. (2017). Fate of microplastics and mesoplastics carried by surface currents and wind waves: A numerical model approach in the Sea of Japan. *Marine Pollution Bulletin*, *121*(1–2), 85–96. https://doi.org/10.1016/j.marpolbul.2017.05.057

Jones, C. E., Dagestad, K.-F., Breivik, Ø., Holt, B., Röhrs, J., Christensen, K. H., … Skrunes, S. (2016). Measurement and modeling of oil slick transport. *Journal of Geophysical Research: Oceans*, *121*, 7759–7775. https://doi.org/10.1002/2016JC012113

Kukulka, T., Proskurowski, G., Morét-Ferguson, S., Meyer, D. W., & Law, K. L. (2012). The effect of wind mixing on the vertical distribution of buoyant plastic debris. *Geophysical Research Letters*, *39*, L07601. https://doi.org/10.1029/2012GL051116

Law, K. L., Morét-Ferguson, S., Maximenko, N. A., Proskurowski, G., Peacock, E. E., Hafner, J., & Reddy, C. M. (2010). Plastic accumulation in the North Atlantic subtropical gyre. *Science*, *329*(5996), 1185–1188.

Laxague, N. J. M., Haus, B. K., Ortiz-Suslow, D. G., Smith, C. J., Novelli, G., Dai, H., Özgökmen, T. M., & Graber, H. C. (2017). Passive optical sensing of the near-surface wind-driven current profile. *Journal of Atmospheric and Oceanic Technology*, *34*(5), 1097–1111. https://doi.org/10.1175/JTECH-D-16-0090.1

Le Hénaff, M., Kourafalou, V. H., Paris, C. B., Helgers, J., Aman, Z. M., Hogan, P. J., & Srinivasan, A. (2012). Surface evolution of the deepwater horizon oil spill patch: Combined effects of circulation and wind-induced drift. *Environmental Science and Technology*, *46*(13), 7267–7273. https://doi.org/10.1021/es301570w

Lumpkin, R., Özgökmen, T. M., & Centurioni, L. (2017). Advances in the application of surface drifters. *Annual Review of Marine Science*, *9*(1), 59–81. https://doi.org/10.1146/annurev-marine-010816-060641

Lund, B., Graber, H. C., Tamura, H., Collins, C. O., & Varlamov, S. M. (2015). A new technique for the retrieval of near-surface vertical current shear from marine X-band radar images. *Journal of Geophysical Research: Oceans*, *120*, 8466–8486. https://doi.org/10.1002/2015JC010961

Matthews, J. P., Ostrovsky, L., Yoshikawa, Y., Komori, S., & Tamura, H. (2017). Dynamics and early post-tsunami evolution of floating marine debris near Fukushima Daiichi. *Nature Geoscience*, *10*, 598–603. https://doi.org/10.1038/NGEO2975

Maximenko, N., Hafner, J., & Niiler, P. (2012). Pathways of marine debris derived from trajectories of Lagrangian drifters. *Marine Pollution Bulletin*, *65*(1), 51–62. https://doi.org/10.1016/j.marpolbul.2011.04.016

Novelli, G., Guigand, C., Cousin, C., Ryan, E., Laxague, N. J. M., Dai, H., … Ozgokmen, T. M. (2017). A biodegradable surface drifter for ocean sampling on a massive scale. *Journal of Atmospheric and Oceanic Technology*. https://doi.org/10.1175/JTECH-D-17-0055.1

Plant, W. J., & Wright, J. W. (1980). Phase speeds of upwind and downwind traveling short gravity waves. *Journal of Geophysical Research*, *85*(C6), 3304–3310. https://doi.org/10.1029/JC085iC06p03304

Reisser, J., Slat, B., Noble, K., Plessis, K. Du, Epp, M., Proietti, M., … Pattiaratchi, C. (2015). The vertical distribution of buoyant plastics at sea: An observational study in the North Atlantic Gyre. *Biogeosciences*, *12*, 1249–1256. https://doi.org/10.5194/bg-12-1249-2015

Stokes, G. G. (1847). On the theory of oscillatory waves. *Transactions Cambridge Philosophical Society*, *8*, 441–473.

Sutherland, P., & Melville, W. K. (2013). Field measurements and scaling of ocean surface wave-breaking statistics. *Geophysical Research Letters*, *40*, 3074–3079. https://doi.org/10.1002/grl.50584

Sutherland, P., & Melville, W. K. (2015). Field measurements of surface and near-surface turbulence in the presence of breaking waves. *Journal of Physical Oceanography*, *45*(4), 943–965. https://doi.org/10.1175/JPO-D-14-0133.1

Webb, A., & Fox-Kemper, B. (2015). Impacts of wave spreading and multidirectional waves on estimating Stokes drift. *Ocean Modelling*, *96*, 49–64. https://doi.org/10.1016/j.ocemod.2014.12.007

Wolfe, D. A., Hameedi, M. J., Galt, J., Watabayashi, G., Short, J., O'Claire, C., … Sale, D. (1994). The fate of the oil spilled from the Exxon Valdez. *Environmental Science and Technology*, *28*(13), 561–568.

Wright, S. L., Thompson, R. C., & Galloway, T. S. (2013). The physical impacts of microplastics on marine organisms: A review. *Environmental Pollution*, *178*, 483–492. https://doi.org/10.1016/j.envpol.2013.02.031

Wu, J. (1983). Sea-surface drift currents induced by wind and waves. *Journal of Physical Oceanography*, *13*(8), 1441–1451. https://doi.org/10.1175/1520-0485(1983)013<1441:SSDCIB>2.0.CO;2

Zappa, C. J., Banner, M. L., Schultz, H., Corrada-Emmanuel, A., Wolff, L. B., & Yalcin, J. (2008). Retrieval of short ocean wave slope using polarimetric imaging. *Measurement Science and Technology*, *19*(5), 055503. https://doi.org/10.1088/0957-0233/19/5/055503